https://doi.org/10.1016/j.ijrmhm.2016.05.005

Effects of binder addition on the surface generation mechanism of WC/Co during high spindle speed grinding (HSSG)

Quanli Zhang[1,2], Suet To[1*], Qingliang Zhao[2], Bing Guo[2] and Mingtao Wu[2]

[1] State Key Laboratory of Ultra-precision Machining Technology, The Hong Kong Polytechnic University, Hong Kong

[2] Centre for Precision Engineering, School of Mechatronics Engineering, Harbin Institute of Technology, Harbin, 150001, China

*Corresponding Author / E-mail: *sandy.to@polyu.edu.hk*, TEL: +852-2766 6587, FAX: +852-2764 7657

Abstract

High spindle speed grinding (HSSG) of WC/Co and binderless WC was conducted to study the effects of binder addition on surface generation mechanism. To help to explain the role of Co binder, Vickers-indentation and nano-indentation test were also conducted on the polished WC/Co and binderless WC workpiece. The indentation results firstly showed that even though the addition of Co binder could obviously improve the toughness of bulk materials, non-uniform surface plastic deformation can be induced by the varied hardness of composing phases in nanoscale, indicated by the shape of load-displacement curves at low loads.. Moreover, except for the scratching grooves and feed marks, the machined WC/Co surface was covered by randomly distributed micro-pits resulted from the dislodgement of hard particles in comparison with the binderless WC. Fast Fourier Transform (FFT) analysis confirmed the obvious contribution of these micro-pits to the spatial frequency at 148.1 1/mm than the feed component. Moreover, the results showed that the machined surface experienced no evident oxidation with minimum quantity lubrication, but a deformed surface layer formed under the dynamic pressure of the

diamond grits during grinding.

Keywords: High spindle speed grinding; Indentation; Co binder; WC; Surface generation

1. Introduction

Tungsten carbide (WC) is extensively used in optical molding industries for its excellent mechanical properties at high temperature, such as high stability, corrosion resistance, high strength and hardness [1, 2]. To improve the toughness and densify WC bulk materials, a certain amount of cobalt (Co) is added as binder for its high temperature stability and good ductility [3-5], and the inter-diffusion of liquid Co and carbon during sintering could promote the interface strength between WC and Co [6], so the mechanical properties of bulk WC/Co materials could be obviously improved.

As is well known, the material microstructure plays a critical role on its mechanical properties and machinability, so it is certain that the material removal and surface generation mechanism of WC/Co under indentation and abrasive machining should have been changed accordingly after the addition of Co. A number of relative investigations have been conducted to study the influence of materials microstructure on the surface damage mechanism of WC/Co carbides. Blanda et al [7] reported that the addition of Co resulted in the appearance of 'mix-mode' indents, where the indents were always at multi-phase points, so great difference of measured hardness was obtained. Duszová et al [8] even found that the higher volume fraction of binder would change the damage mechanism of WC/Co from fracture of WC/WC bridges to deformation of Co binder under indentation. Then, it can be drawn that the critical load could be improved and ductile material removal mode could be achieved more easily during grinding [9]. The existing phase boundaries between WC and Co would impede the propogation of interfacial micro-cracks which resulted in the grains dislodgement, and the strengthening effects of binders has been proved by Zhang et al [4]. Moreover, Yin et al [10] found that the grinding surface of WC/Co was

characterized by microgrooves and plastic flow regions via slip of WC grains along the Co binder. More recently, Gant et al [11, 12] also reported the close relation of wear modes with material microstructure for WC/Co. Binder extrusion and fragmented tungsten carbide grains embedded in binders under the single point abrasion experiments could be induced [13], which also limited the surface finish achieved [14]. It has been reported that the very nature of the damage behavior of ceramics could be changed and optimized by the addition of binders [15], and the mechanics under varied mechanical loading still need further investigation.

In the present work, nanoindentation and Vickers-hardness indentation test was firstly performed to study and analyze the different material damage mechanisms which were focused on the effects of binders' addition. Then, the role of Co on the surface damage mechanism of WC/Co under high spindle speed grinding (HSSG) was investigated. To specify the influence of Co, Vickers indentation and high spindle speed grinding (HSSG) of binderless WC material were also performed for comparison.

2. Experiments

2.1 Materials and machine

Commercially available WC/Co carbides (~6.wt% Co, Goodfellow Cambridge Ltd., UK) and binderless WC (Dijet Industrial Co., Ltd., Japan) were used. Before the indentation test, the workpiece materials were firstly polished with diamond paste of 1 μm diameter to remove the surface layer and reduce the impact of the original surface defects, with the obtained surface roughness (R_a) to be about 3 nm for the workpiece. The surface morphology of the polished WC/Co composites indicates that there exists no obvious defects in the original bulk materials and the WC grain size is about 2 μm, as can be seen from Fig. 1(a) and (b). Nanoindentation test was

conducted on a nano-indenter (Nano-Indenter® XP system, MTS) with continuous stiffness measurement (CSM) mode at varied parameters. The Vickers indentation test was conducted on the polished surface by Vickers micro-hardness tester (MicroWiZhard) under the loads of 0.2 kg, with the loading time of 5 s, holding time of 10 s and unloading time 5 s. Three repeated times of indentation were performed for both WC/Co and binderless WC at varied surface positions to investigate the surface profile generated under quasi-static normal pressure. High spindle speed grinding (HSSG) was conducted on Moore Nanotech 450UPL, detail illustration of the grinding setup and mechanical properties of WC/Co and binderless WC composites could be found in [16] and [2]. The grinding parameters in the present work are listed in Table 1.

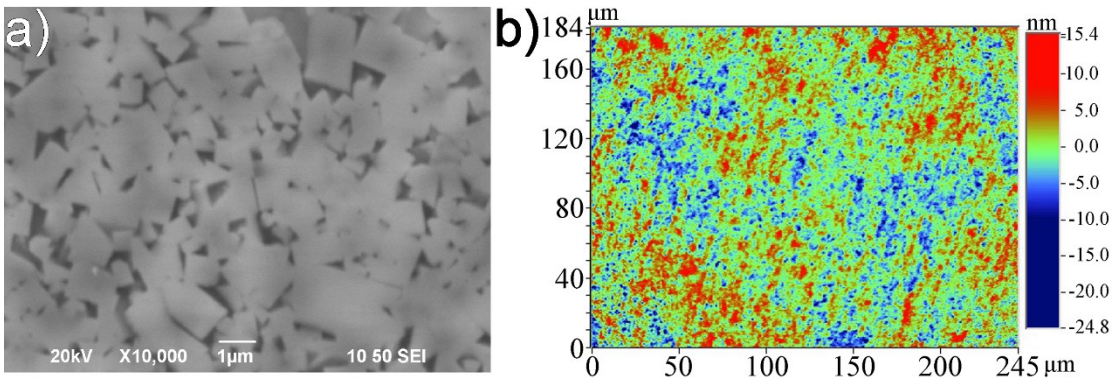

Fig. 1 (a) SEM morphology, (b) 3D topography of the polished WC/Co composites

Table 1. Micro-grinding parameters

Wheel(20mm in diameter)	1500#G0787B195
Wheel *RPM* (rpm)	20,000
Workpiece *RPM* (rpm)	120
Depth of cut (μm)	0.5
Feed rate (mm/min)	0.5
Coolant	CLAIRSOL 350
Workpiece size	10×10×5 mm

2.2 Characterization and measurement

The surface morphology of the indentation imprints were characterized by scanning electron microscope with backscattered electron imaging (BSEM, Hitachi TM3000). The polished and grinding surface morphology of WC/Co were examined by a scanning electron microscope

equipped with EDS (SEM, JEOL Model JSM-6490). Besides, the polished and grinding surfaces were analyzed by the white light interferometers (WLI, WYKO NT8000 and ZYGO Lamda Nexview) and atomic force microscope (AFM, Park's XE-70). X-ray diffraction (XRD, Rigaku SmartLab) with *CuKα* radiation (45 kV, 200mA) was also performed to analyze the polished and grinding WC/Co surface in a scanning angle range of 25 to 50 °, and focused ion beam (FIB, JEOL Model JIB-4501) was utilized to examine the machined surface.

3. Results and discussion

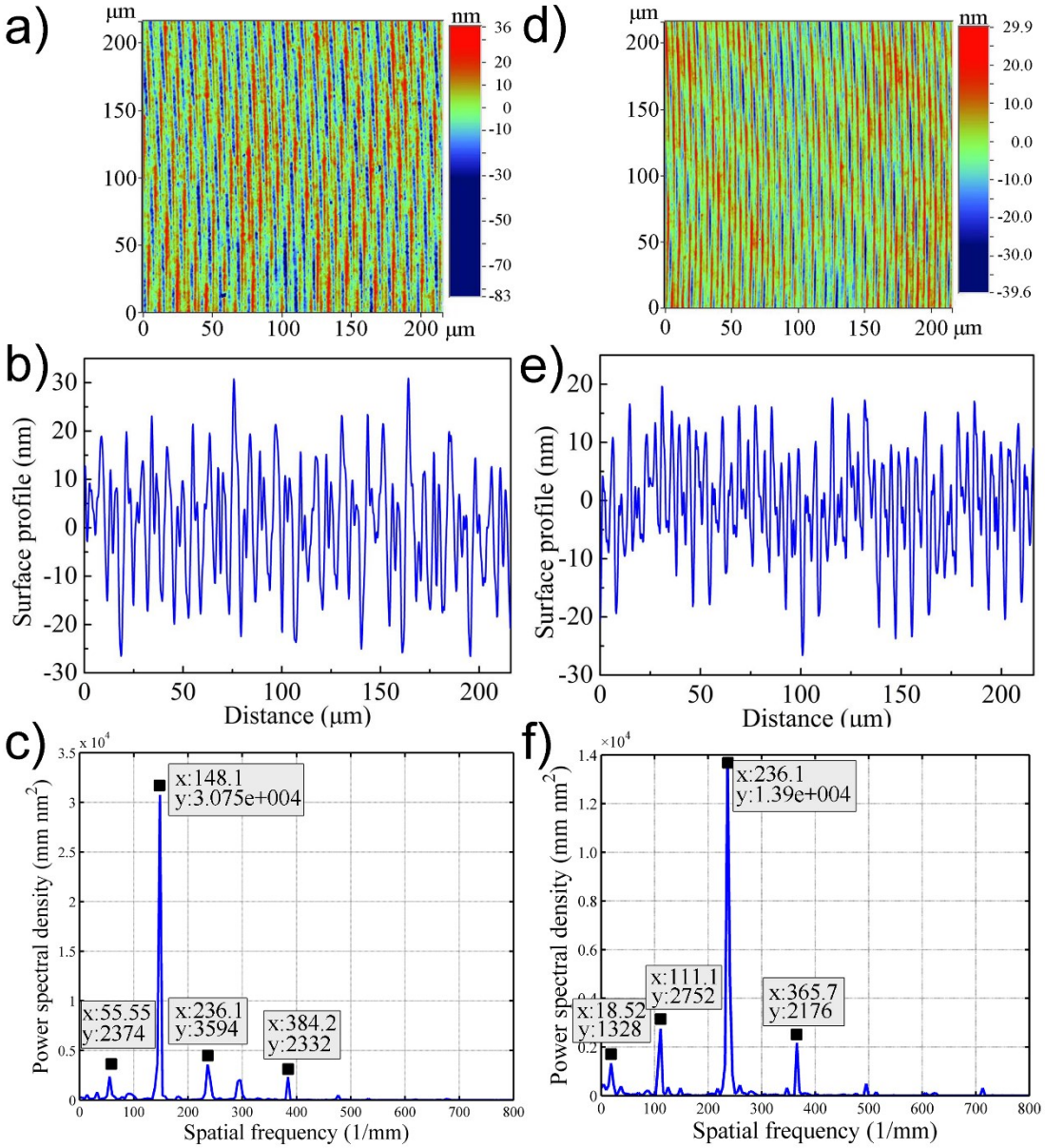

Fig .2 Surface topography, cross-sectional profile height and FFT results of the machined surface: (a), (b) and (c) for WC/Co; (d), (e) and (f) for binderless WC

Fig. 2(a) and (d) shows the surface topography of WC/Co and binderless WC after grinding, which was measured at the position of 4 mm from the workpiece center. It could be found that the machined surface of both WC/Co and binderless WC were covered by obvious feed marks. However, things also differed because many superficial micro-pits occurred on WC/Co surface, which is shown in Fig. 3(a). On the one hand, the hard WC particles were extruded to be denser under the shock pressure of diamond grits for WC/Co, and some WC particles would fall as the extruded Co between the neighboring hard phases was removed with less binders remained, leaving some pits on the surface. On the other hand, due to the different harness between WC and Co, the material removal rate differed, resulting in the varied height between WC particles and cobalt binders. In the previous study, it was found that cobalt binder had great impact on the fatigue life [17]. Under the cyclic scratching pressure of diamond grits during high spindle speed grinding (HSSG), the cobalt binder will be extruded and removed, resulting in the dislodgement of WC grains [18, 19]. The cross sectional profile height of the machined surface at 4 mm from the workpiece center, as is shown in Fig. 2(b) and (e), indicates the worse surface finish obtained for WC/Co. The surface roughness (R_a) is 9.42 nm for WC/Co and 7.25 nm for binderless WC, respectively. The results of Fast Fourier Transform (FFT) analysis confirmed the great influence of micro-pits generated on the machined surface. As can be seen from Fig. 2(c) and (f), the main spatial frequency for WC/Co is located at 148.1 1/mm, while the main peak is 236.1 1/mm for binderless WC, which corresponds to the feed components calculated based on the Eq.(1)

$$f_{spatial} = \frac{1}{d_{pp} \times 10^{-3}} \tag{1}$$

where d_{pp} is the measured distance between the waviness peaks (μm), and $f_{spatial}$ is the spatial frequency (1/mm). Therefore, even though the Co binder could improve the toughness of bulk WC/Co materials, the impact on the surface generation mechanism during high spindle speed grinding (HSSG) should be paid more attention. As has been indicated by the nanoindentation test above, the different hardness of the bulk material composition phases would lead to the varied penetration depth for diamond grit, so the material removal rate also differed. Especially for the ductile Co, it will be extruded under the dynamic pressure of diamond grits [19]. Then, the extruded Co could be removed by the following diamond grits, leaving many micro-pits on the machined surface [13]. Moreover, as another material removal mode, the WC grain dislodgement could be induced [18]. These both contributed to the main spatial frequency (148.1 1/mm), which resulted in the obtained surface roughness (R_a) higher than binderless WC.

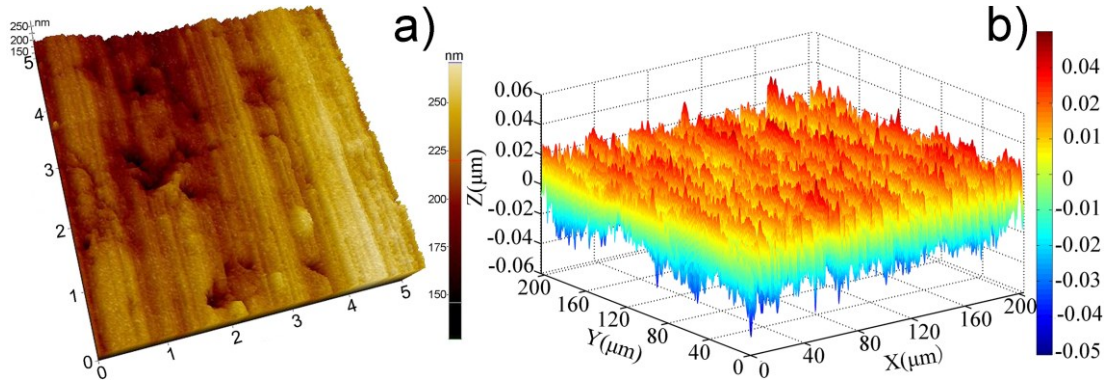

Fig. 3 3D surface topography of the machined WC/Co surface measured by: (a) AFM; (b) WLI

Considering the fine grinding parameters and the random protrusion height of diamond grits, nanoindentation was used to explain the mechanical behavior difference in WC particles and Co binder. Fig. 4(a) and (b) shows the load-displacement curves of nanoindentation for WC/Co under the loading/unloading time of 5 s and varied loads. It could be found that the load-displacement curve at 5 mN is obviously crooked, and there exists a fast displacement zone at the initial point which results in an even flat load-displacement curve. Previous studies have reported that not only

the crystallographic orientation of WC particles but also the Co binder addition contributed to this phenomenon [7, 20, 21]. Moreover, it could be found that the “pop-in” effect at the lower load and loading rate is more obvious than higher load and loading rate. As far as the contact area is concerned, the protrusion height of the scratched grooves promoted the rapid displacement at a low loading rate, which is shown in Fig. 3(b). In addition, the pop-in phenomenon did not obviously appeared for the machined surface at the initial loading stage, which is attributed to the formation of a densified and deformed layer induced by grinding [22, 23].

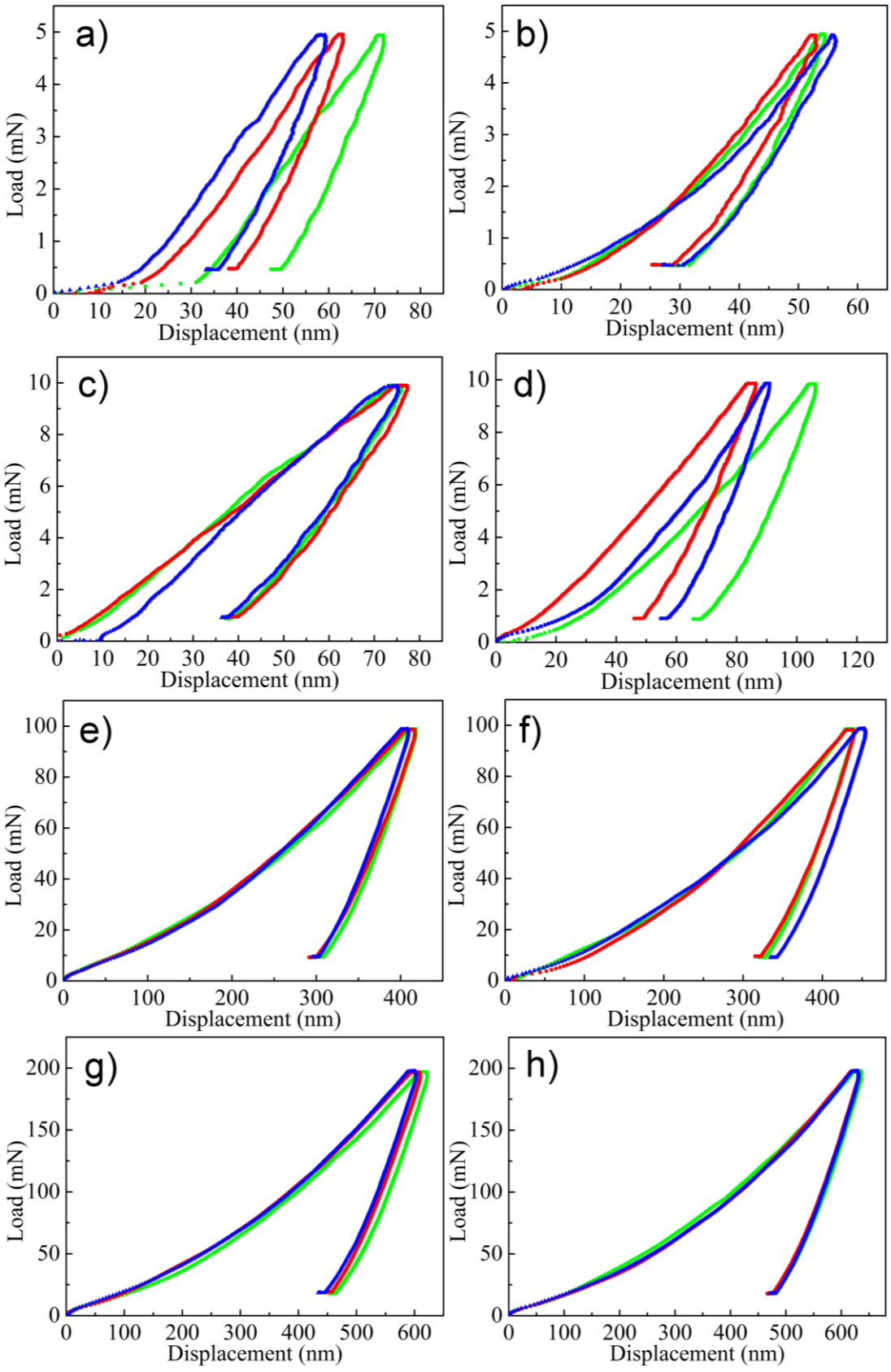

Fig. 4 Load-displacement curves for WC-Co before and after grinding at the max loads of 5 mN, 10 mN, 100 mN and 200 mN: (a), (c), (e) and (g) for polished surface; (b), (d), (f) and (h) for grinding surface

However, with the increase of maximum load, the curves at different positions were reproducible. This could be attributed to the indentation size effects (ISE) [24, 25]. To further illustrate this problem, the measured elastic modulus and hardness by nanoindentation at varied loads for the polished and machined surface are shown in Fig. 5. After the addition of binders, the varied mechanical properties between the hard particles and binders would result in the non-regular load-displacement curves at different positions. At the load of 5 mN, the plastic deformation of Co binder in WC/Co will be firstly induced, leading to the quick displacement at the beginning, even though the nanoindentation was performed on WC particle. With the increase of load, the higher load rate at 10 mN and 25 mN will make the Co binder around WC particle deformed quickly, resulting in the higher dynamic toughness and geometrically necessary dislocations (GNDS) strengthening effects [24]. This is in consistence with the result that single WC grains were plastically deformed by slip during grinding process [13, 23]. However, the strengthening effects of GNDS was limited with the further rise of the max load, as the length of deformation became much greater than the grain size. Therefore, the measured modulus and hardness firstly increased and then stay steady. Moreover, it can be easily seen that the measured hardness and modulus for the machined surface are all slightly smaller than the polished surface. In fact, a hardening surface layer with compressive residual stress was reported during the diamond grinding of WC/Co [23]. In the present work, the reduced hardness and modulus can be attributed the worsening surface finish and scratched grooves which could be deformed under the indentation pressure, resulting in a higher penetration depth.

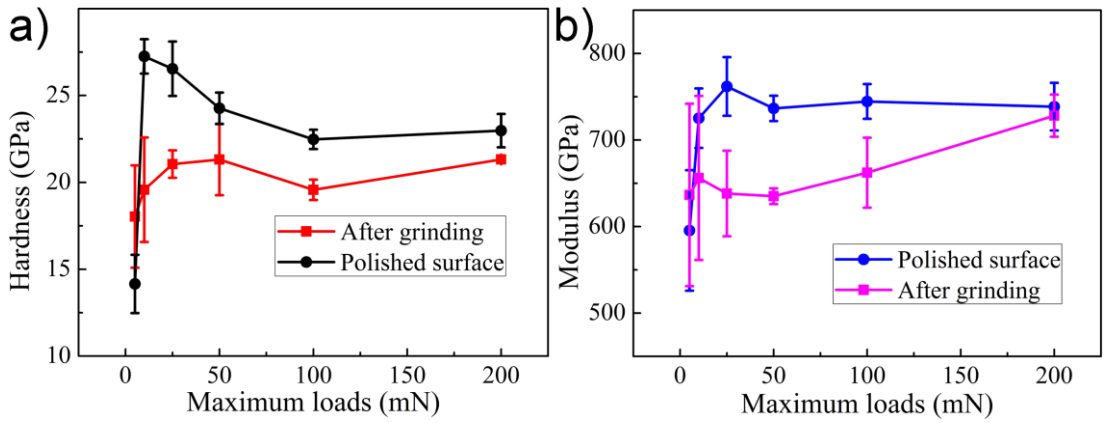

Fig. 5 (a) Hardness and (b) elastic modulus of WC/Co measured by nano-indentation at varied max loads

Previous studies have shown that the grinding force in micro-grinding could reach 2 N [26], so Vickers-hardness indentation under 0.2 kgf is performed to illustrate the surface damage mechanism of WC/Co under grinding, with the contact area between diamond wheel and workpiece considered as a whole. Fig. 6 shows the surface morphology of the Vickers-indentation imprints on WC/Co and binderless WC. As can be seen from Fig. 6(a), only regular indentation imprints were replicated from the shape of Vickers indenter on WC/Co surface under the load of 0.2 kg, and there was no obvious surface crack generated near the indentation position. More specifically, the workpiece material was extruded and swelled out under the pressure of indenter, resulting in the plastic deformation for both WC and Co. Besides, an obvious densified region could be found on the compressed surface. For binderless WC at the same loading force, as is shown in Fig. 6(b), obvious radial cracks could be observed around the four sharp tips. Therefore, it can be safely drawn that the addition of Co binder could obviously improve the toughness of bulk materials.

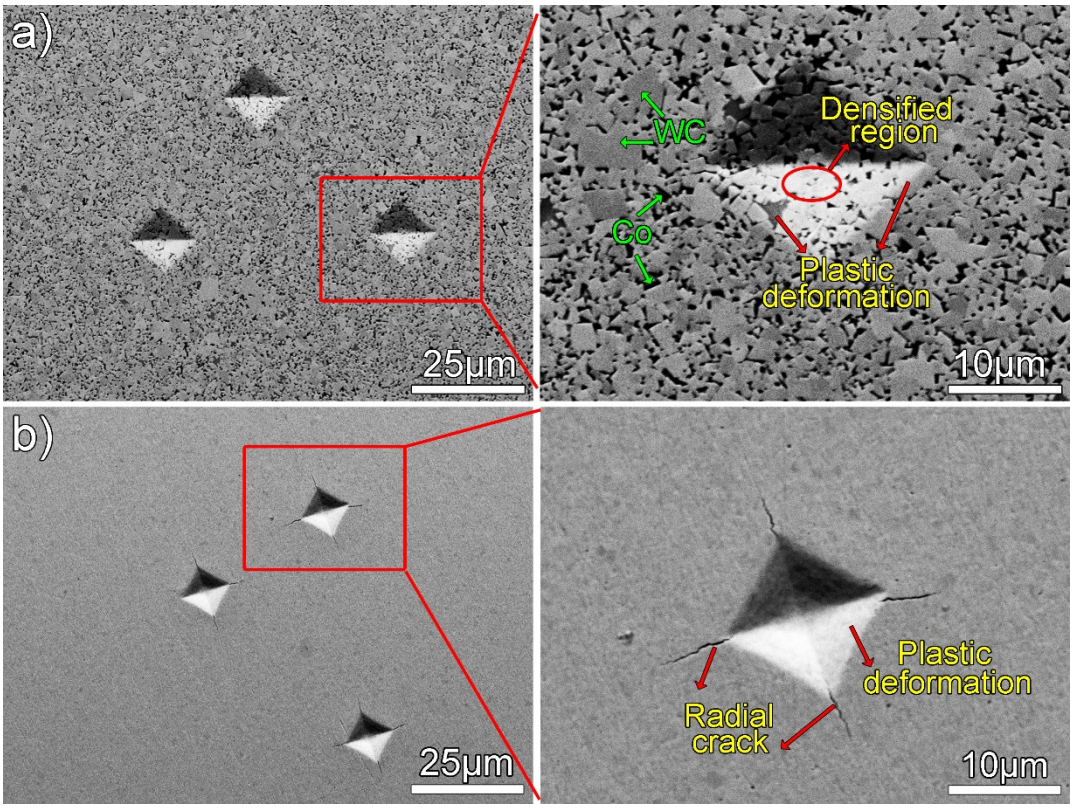

Fig. 6 BSEM morphology of Vickers-hardness indentation imprints at the load of 0.2 kg: (a) WC/Co, (b) binderless WC

To reveal the toughening mechanism, the surface morphology of indentation imprints for WC/Co and binderless WC under 5 kg is shown in Fig. 7. Obvious transgranular and interphase cracks for WC/Co could be generated under higher load. The twisted cracks for WC/Co indicates that the toughness (K_c) could be improved as the interfaces bridging between WC particles and Co binders could impeded the propagation of cracks [27]. According to [15, 28-30], micro-cracking toughening mechanism was well established for ceramic-composites, as is indicated by the green arrows in Fig. 7(a). In these studies, the role of the weak interfaces has been identified. Specifically for the cemented WC/Co carbides, the plastic deformation of cobalt binder during cracks formation and the phase transformation from f.c.c to h.c.p plays an important role on the toughening of WC/Co [31, 32]. In addition, due to the irregular shapes of WC particles [33], as is

shown in Fig. 1(a), stress concentration could be induced at the boundaries between WC and Co, so it could be readily seen that the origin of cracks was right at the phase boundaries. Presumably, the micro-cracking at the phase boundaries would also promote the WC grains dislodgement.

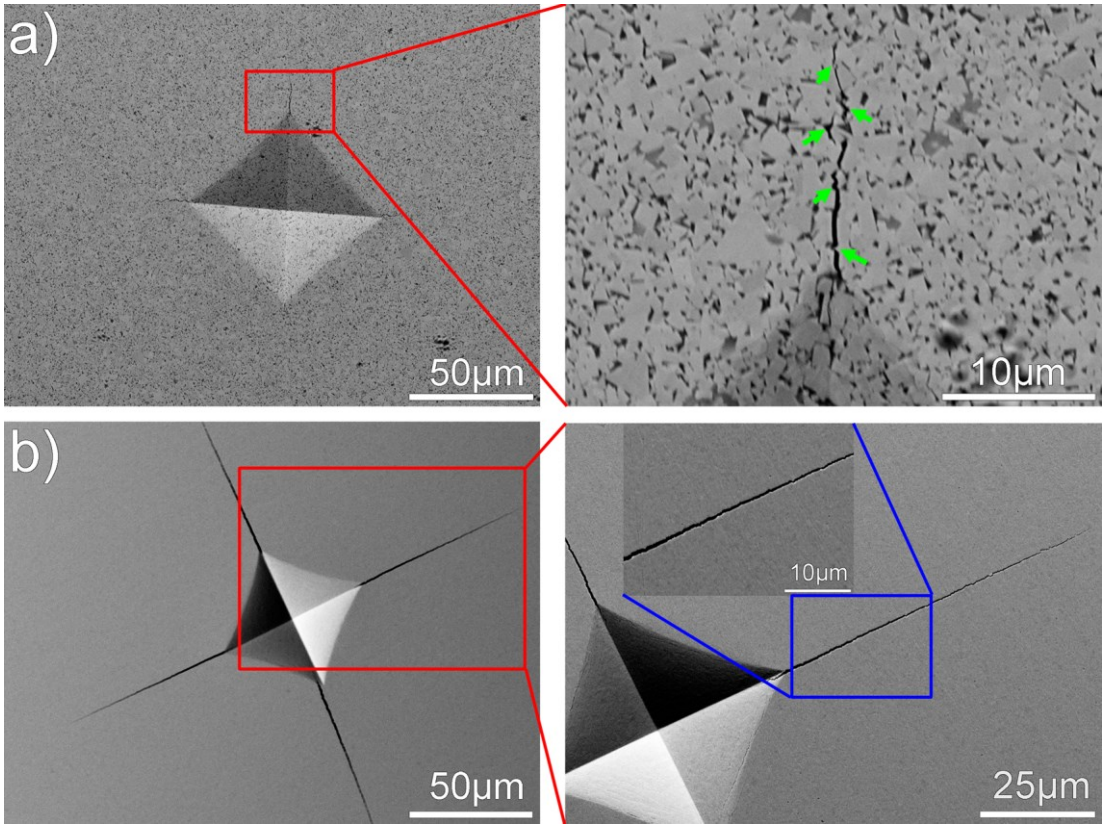

Fig. 7 Surface morphology of Vickers-hardness indentation imprints at the load of 5 kg on: (a) WC/Co, (b) binderless WC

Fig. 8 shows the surface morphology and the element composition of the WC/Co workpiece after grinding. It can be easily seen that no obvious oxidation occurred on the machined surface for both WC particle and the binders with the minimum quantity lubrication (MQL). Nevertheless, the XRD pattern of the machined surface, as is illustrated in Fig. 9, shows some changes in the peak intensity. This is attributed to the formation of a seriously deformed layer on the grinding surface [22, 23], which is also identified in the present work, shown in Fig. 9(b). Under the dynamic pressure of the diamond grits during high spindle speed grinding (HSSG), Co can be

extruded and the mean free path between neighboring WC grains decreased. Moreover, amorphization of WC could be induced under the shear stress of dynamic diamond grits scratching, which has been reported by Stoyanov et al. [34].

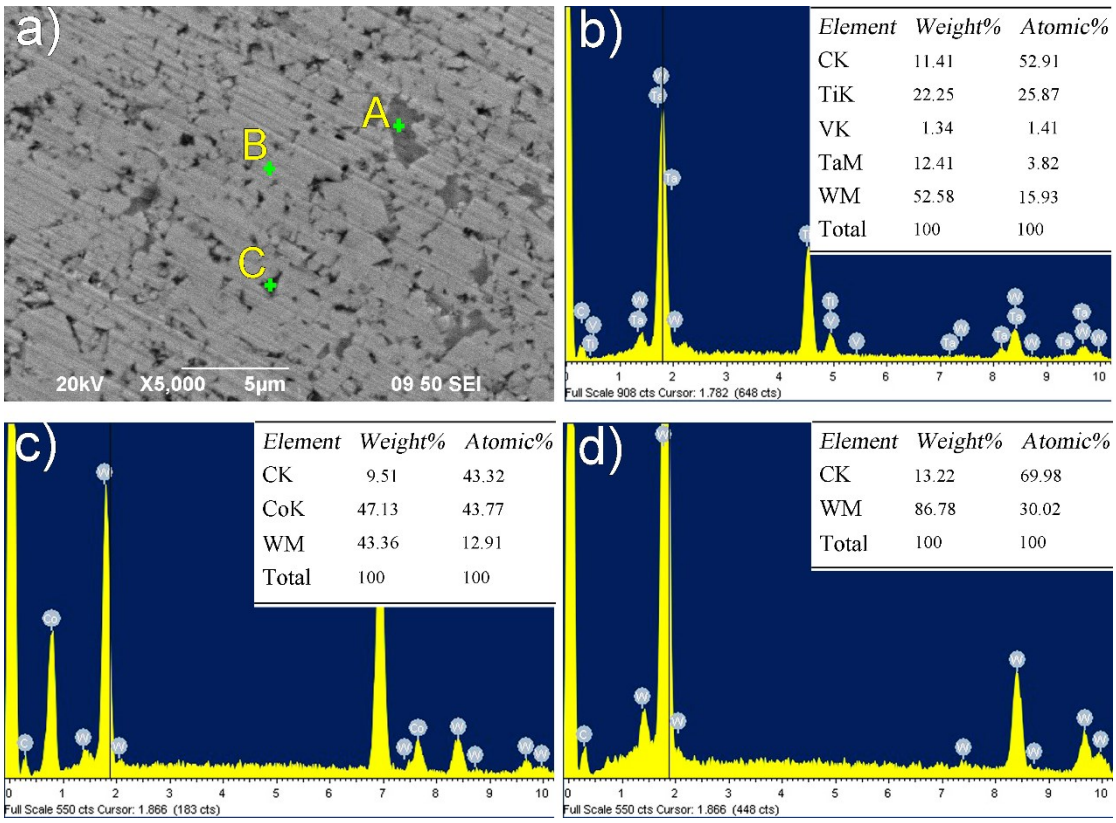

Fig. 8 SEM morphology and EDS results of the machined WC/Co surface

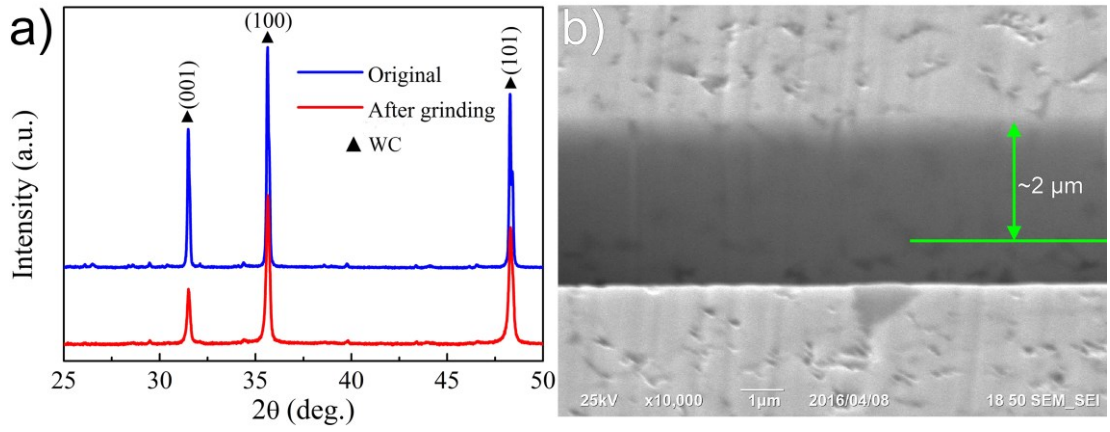

Fig. 9 (a) XRD pattern of the original material and machined surface; (b) FIB section of the machined surface

4. **Conclusions**

The main aim of present study was to investigate the effects of binder (Co) addition on the

surface generation mechanism of WC/Co carbide during high spindle speed grinding (HSSG). The following conclusions could be drawn:

(1) Even though Co binder addition could improve the toughness (K_c) of bulk materials evidently, it deteriorates the surface finish of WC/Co (R_a=9.42 nm) achieved during high spindle speed grinding (HSSG), compared with binderless WC (R_a=7.25 nm);

(2) The inconsistent loading-displacement curves of nano-indentation at low loads results from the varied mechanical properties of WC basal plane, prismatic plane and Co binder, while the large contact scale at higher loads contributes to the reproducible curves. So the material removal rate between WC grains and Co binder during grinding differed under the dynamic pressure of diamond grits;

(3) Under the dynamic pressure of diamond grits, hard particle dislodgement occurred as another material removal mode due to the non-uniform material removal of WC grains and the extrusion of Co binder, leading to the generation of many micro-pits on the machined surface of WC/Co, which contributes to the spatial frequency at 148.1 1/mm;

(4) No obvious oxidation occurred for WC/Co under high spindle speed grinding (HSSG) with minimum quantity lubrication (MQL), but a deformed layer of about 2 μm formed on the machined surface with the extrusion of Co, resulting in the decreasing peak intensity of X ray diffraction.

Acknowledgement

The work was partially supported by the Research Committee of the Hong Kong Polytechnic University (RTRA) and also the National Natural Science Foundation of China (NSFC) (Project No.:51475109).

References

[1] H.Q. Sun, R. Irwan, H. Huang, G.W. Stachowiak, Surface characteristics and removal mechanism of cemented tungsten carbides in nanoscratching, Wear, 268(2010) 1400-1408.

[2] B. Guo, Q. Zhao, M. Jackson, Precision grinding of binderless ultrafine tungsten carbide (WC) microstructured surfaces, The International Journal of Advanced Manufacturing Technology, 64(2013) 727-735.

[3] Z.Z. Fang, X. Wang, T. Ryu, K.S. Hwang, H.Y. Sohn, Synthesis, sintering, and mechanical properties of nanocrystalline cemented tungsten carbide-A review, International Journal of Refractory Metals and Hard Materials, 27(2009) 288-299.

[4] L. Zhang, Z. Wang, S. Chen, T. Xu, J. Zhu, Y. Chen, Binder phase strengthening of WC-Co alloy through post-sintering treatment, International Journal of Refractory Metals and Hard Materials, 50(2015) 31-36.

[5] D. Han, J.J. Mecholsky. Jr, Fracture analysis of cobalt-bonded tungsten carbide composites, Journal of Materials Science, 25(1990) 4949-4956.

[6] O. Eso, Z.Z. Fang, A. Griffo, Kinetics of cobalt gradient formation during the liquid phase sintering of functionally graded WC-Co, International Journal of Refractory Metals and Hard Materials, 25(2007) 286-292.

[7] M. Bľanda, A. Duszová, T. Csanádi, P. Hvizdoš, F. Lofaj, J. Dusza, Indentation hardness and fatigue of the constituents of WC-Co composites, International Journal of Refractory Metals and Hard Materials, 49(2015) 178-183.

[8] A. Duszová, P. Hvizdoš, F. Lofaj, Ł. Major, J. Dusza, J. Morgiel, Indentation fatigue of WC-Co cemented carbides, International Journal of Refractory Metals and Hard Materials, 41(2013)

229-235.

[9] T.G. Bifano, T.A. Dow, R.O. Scattergood, Ductile-regime grinding: A new technology for machining brittle materials, Journal of Manufacturing Science and Engineering, 113 (1991) 184-189.

[10] L. Yin, A.C. Spowage, K. Ramesh, H. Huang, J.P. Pickering, E.Y.J. Vancoille, Influence of microstructure on ultraprecision grinding of cemented carbides, International Journal of Machine Tools and Manufacture, 44(2004) 533-543.

[11] A.J. Gant, M.G. Gee, Wear modes in slurry jet erosion of tungsten carbide hardmetals: Their relationship with microstructure and mechanical properties, International Journal of Refractory Metals and Hard Materials, 49(2015) 192-202.

[12] A.J. Gant, M.G. Gee, B. Roebuck, Rotating wheel abrasion of WC/Co hardmetals, Wear, 258(2005) 178-188.

[13] A.J. Gant, M.G. Gee, D.D. Gohil, H.G. Jones, L.P. Orkney, Use of FIB/SEM to assess the tribo-corrosion of WC/Co hardmetals in model single point abrasion experiments, Tribology International, 68 (2013) 56-66.

[14] M. Yahiaoui, J.Y. Paris, J. Denape, A. Dourfaye, Wear mechanisms of WC-Co drill bit inserts against alumina counterface under dry friction: Part 1-WC-Co inserts with homogenous binder phase content, International Journal of Refractory Metals and Hard Materials, 48 (2015) 245-256.

[15] B.R. Lawn, N.P. Padture, H. Cai, F. Guiberteau, Making ceramics "Ductile", Science, 263 (1994) 1114-1116.

[16] Q. Zhang, S. To, Q. Zhao, B. Guo, G. Zhang, Impact of material microstructure and diamond grit wear on surface finish in micro-grinding of RB-SiC/Si and WC/Co carbides, International Journal

of Refractory Metals and Hard Materials, 51 (2015) 258-263.

[17] T. Sailer, M. Herr, H.G. Sockel, R. Schulte, H. Feld, L.J. Prakash, Microstructure and mechanical properties of ultrafine-grained hardmetals, International Journal of Refractory Metals and Hard Materials, 19 (2001) 553-559.

[18] Q. Zhang, S. To, Q. Zhao, B. Guo, Surface generation mechanism of WC/Co and RB-SiC/Si composites under high spindle speed grinding (HSSG), International Journal of Refractory Metals and Hard Materials, 56 (2016) 123-131.

[19] Q. Zhang, S. To, Q. Zhao, B. Guo, Surface damage mechanism of WC/Co and RB-SiC/Si composites under high spindle speed grinding (HSSG), Materials & Design, 92 (2016) 378-386.

[20] A. Duszová, R. Halgaš, M. Bľanda, P. Hvizdoš, F. Lofaj, J. Dusza, J. Morgiel, Nanoindentation of WC-Co hardmetals, Journal of the European Ceramic Society, 33 (2013) 2227-2232.

[21] J.J. Roa, E. Jimenez-Pique, C. Verge, J.M. Tarragó, A. Mateo, J. Fair, L. Llanes, Intrinsic hardness of constitutive phases in WC-Co composites: Nanoindentation testing, statistical analysis, WC crystal orientation effects and flow stress for the constrained metallic binder, Journal of the European Ceramic Society, 35 (2015) 3419-3425.

[22] J. Yang, M. Odén, M.P. Johansson-Jõesaar, L. Llanes, Grinding effects on surface integrity and mechanical strength of WC-Co cemented carbides, Procedia CIRP, 13 (2014) 257-263.

[23] J.B.J.W. Hegeman, J.T.M. De Hosson, G. de With, Grinding of WC–Co hardmetals, Wear, 248 (2001) 187-196.

[24] G.Z. Voyiadjis, R. Peters, Size effects in nanoindentation: an experimental and analytical study, Acta Mechanica, 211 (2009) 131-153.

[25] A.H. Almasri, G.Z. Voyiadjis, Nano-indentation in FCC metals: experimental study, Acta

Mechanica, 209 (2009) 1-9.

[26] P. Lee, J. Nam, C. Li, S. Lee, An experimental study on micro-grinding process with nanofluid minimum quantity lubrication (MQL), International Journal of Precision Engineering and Manufacturing, 13 (2012) 331-338.

[27] B.R. Lawn, Fracture of brittle solids, New York : Cambridge University Press, 1993.

[28] L.S. Sigl, Microcrack toughening in brittle materials containing weak and strong interfaces, Acta Materialia, 44 (1996) 3599-3609.

[29] L.S. Sigl, H. Kleebe, Microcracking in B4C-TiB2 Composites, Journal Of The American Ceramic Society, 78 (1995) 2374-2380.

[30] M. Rühle, A.G. Evans, R.M. McMeeking, P.G. Charalambides, J.W. Hutchinson, Microcrack toughening in alumina/zirconia, Acta Metallurgica, 35 (1987) 2701-2710.

[31] U. Schleinkofer, H.G. Sockel, K. Go Rting, W. Heinrich, Microstructural processes during subcritical crack growth in hard metals and cermets under cyclic loads, Materials Science and Engineering: A, 209 (1996) 103-110.

[32] L.S. Sigl, H.E. Exner, Experimental study of the mechanics of fracture in WC-Co alloys, Metallurgical Transactions A, 18 (1987) 1299-1308.

[33] S. Chang, P. Chang, Investigation into the sintered behavior and properties of nanostructured WC-Co-Ni-Fe hard metal alloys, Materials Science and Engineering: A, 606(2014) 150-156.

[34] P. Stoyanov, P.A. Romero, T.T. Järvi, L. Pastewka, M. Scherge, P. Stemmer, A. Fischer, M. Dienwiebel, M. Moseler, Experimental and Numerical Atomistic Investigation of the Third Body Formation Process in Dry Tungsten/Tungsten-Carbide Tribo Couples, Tribology Letters, 50 (2013) 67-80.